Earth and Planetary Science Letters 284 (2009) 527–537

Contents lists available at ScienceDirect

Earth and Planetary Science Letters

journal homepage: www.elsevier.com/locate/epsl

The origin of high-MgO diamond eclogites from the Jericho Kimberlite, Canada

Katie A. Smart [a,*], Larry M. Heaman [a], Thomas Chacko [a], Antonio Simonetti [a,1], Maya Kopylova [b], Dale Mah [c,2], Delene Daniels [c]

[a] Department of Earth and Atmospheric Sciences, University of Alberta, Edmonton, Alberta, Canada T6G 2E3
[b] Department of Earth and Ocean Sciences, The University of British Columbia, Vancouver, B.C., Canada V6T 1Z4
[c] Tahera Diamond Corporation, Canada

ARTICLE INFO

Article history:
Received 12 January 2009
Received in revised form 13 May 2009
Accepted 14 May 2009
Available online 9 July 2009

Editor: R.W. Carlson

Keywords:
diamond-bearing eclogites
mantle metasomatism
trace-element geochemistry
element diffusion
Slave craton
Jericho kimberlite

ABSTRACT

A unique suite of diamond-rich eclogites from the Jericho kimberlite, Nunavut, Canada, has a uniform but unusual geochemical and isotopic composition that is unlike any other eclogite suite worldwide. Compared to other eclogite suites, garnets from Jericho diamond-bearing eclogites have high MgO (19.6–21.2 wt.%), Cr_2O_3 (0.28–0.60 wt.%), Sc (88–113 ppm), and Zr (32–36 ppm) contents and are characterized by consistent highly fractionated chondrite-normalized HREE patterns ($[Lu/Gd]_N = 4.0–6.6$). Na-poor clinopyroxene has a uniform LREE-enriched pattern and radiogenic $^{87}Sr/^{86}Sr$ values between 0.7057 and 0.7061, higher than other eclogite groups at Jericho and the Jericho kimberlite itself. The distinct geochemical and isotopic compositions of the Jericho diamond eclogites are not directly compatible with either the subducted oceanic crust or high-pressure mantle melt models commonly invoked for the origin of mantle eclogites. We propose a multi-stage origin that involves multiple metasomatic events coupled with hybridization between basaltic eclogite and mantle peridotite. Emplacement of basaltic eclogites in the diamond stability field was followed by metasomatism by a carbon-bearing, LREE-enriched metasomatic fluid or melt as recorded by clinopyroxene and diamond inclusions in garnet. Subsequent or concurrent partial melting of eclogite produced melts that facilitated diffusional elemental exchange between residual eclogite and ambient peridotite. This process enabled the eclogites to attain their distinct high-Mg and Cr composition. Finally, carbonatite-like modal metasomatism grew phlogopite, carbonate and apatite and potentially also facilitated additional diamond growth, producing the extreme diamond enrichments found in these eclogites.

© 2009 Elsevier B.V. All rights reserved.

1. Introduction

Although the proportion of eclogite within the cratonic lithospheric mantle is inferred to be small (<2%, Schulze, 1989), the proportion of eclogite xenoliths and eclogitic diamonds recovered from some kimberlites, including the Jericho kimberlite, is surprisingly large (e.g. Stachel and Harris, 2008). Despite the worldwide abundance of eclogitic diamonds, there are comparatively fewer diamondiferous eclogite xenoliths available for study, limiting our understanding of the origin of eclogitic diamonds and their host rocks. Additionally, mantle eclogites can provide insight on the composition and evolution of the continental lithospheric mantle. Two main hypotheses have been proposed for the origin of eclogite xenoliths: 1) remnants of subducted and metamorphosed oceanic crust (e.g. Helmstaedt and Doig, 1975; Jagoutz et al., 1984; MacGregor and Manton, 1986; Jacob et al., 1994; Jacob 2004) and 2) cumulates of basaltic magmas crystallized at high pressure (e.g. O'Hara and Yoder, 1967; Smyth et al., 1989). In this study, we evaluate these hypotheses in light of the major-, trace-element and Sr and Pb isotope compositions of minerals in a suite of high-MgO eclogite xenoliths recently recovered from the Jericho kimberlite, including thirteen spectacularly fresh, diamond-rich eclogites.

1.1. Background

The 173 Ma Jericho kimberlite (Heaman et al., 2006) is located in the northern Slave craton in Nunavut, Canada approximately 400 km NNE of Yellowknife. Our new data and previous studies on Jericho eclogites (Cookenboo et al., 1998; Kopylova et al., 1999a; Heaman et al., 2002; Schmidberger et al., 2005; Heaman et al., 2006) reveal that in addition to garnet and clinopyroxene, Jericho eclogites may also contain diamond, kyanite, corundum, rutile, phlogopite, apatite or zircon. The Jericho eclogites can be subdivided into three broad geochemical groups based on garnet composition; 1) Mg-rich (19.6–21.2 wt.% MgO), 2) Ca-rich (up to 17.5 wt.% CaO), including kyanite-bearing eclogites, and 3) Fe-rich (up to 26.5 wt.% FeO), including zircon-bearing xenoliths. This grouping broadly correlates geochemically with the Group A–B–C eclogite classification originally proposed

* Corresponding author. Tel.: +1 780 271 3452; fax: +1 780 492 2030.
E-mail address: kasmart@ualberta.ca (K.A. Smart).
[1] Dept. Civil Engineering & Geological Sciences, University of Notre Dame, Notre Dame, IN, USA, 46556.
[2] Olivut Resources Ltd.

0012-821X/$ – see front matter © 2009 Elsevier B.V. All rights reserved.
doi:10.1016/j.epsl.2009.05.020

by Coleman et al. (1965), and will be used to describe the three groups hereafter. The diamond-bearing eclogites at Jericho are predominantly Mg-rich Group A eclogites and have homogeneous mineral compositions (Cookenboo et al., 1998; Heaman et al., 2006). A few intermediate-MgO, Group B (~14.0 wt.% MgO) diamond eclogite xenoliths have recently been reported from Jericho by De Stefano et al. (2009). Garnet-clinopyroxene thermometry of the high-MgO diamond eclogites using the calibrations of Ellis and Green (1979) and Krogh Ravna (2000) indicates a restricted temperature range of 1000–1015 °C (calculated at 5.0 GPa) for the last equilibration (Cookenboo et al., 1998; Heaman et al., 2006). This differs from diamond-bearing eclogites from the Diavik kimberlites, just 100 km south of Jericho, which have Group B and C compositions and record much higher temperatures (1127–1299 °C, Schmidberger et al., 2007). The uniform mineral compositions and limited range of equilibration temperatures of the Jericho diamond eclogites led Cookenboo et al. (1998) to propose that these rocks represent high-pressure cumulates from primary mantle melts. This origin is distinct from all other Group B and C eclogites at Jericho, which have been interpreted to be remnants of Paleoproterozoic subducted oceanic crust (Heaman et al., 2002; Schmidberger et al., 2005; Heaman et al., 2006). Although Paleoproterozoic to Mesoproterozoic formation and modification ages have been reported for other suites of Jericho eclogites (Heaman et al., 2002; Schmidberger et al., 2005; Heaman et al., 2006), there is no age information available for the high-MgO, Jericho diamond eclogites.

1.2. Petrography of the Jericho diamond eclogites

The Jericho diamond eclogites (abbreviated JDE hereafter) investigated in this study are dominantly garnet–clinopyroxene–diamond ± phlogopite (1–2%) rocks, where diamond and phlogopite can comprise up to 20% and 2% of the mode, respectively (Fig. 1a). Reddish-orange garnet and vibrant green clinopyroxene occur as 1–3 mm, generally fresh inclusion-free crystals with a granoblastic texture. These rocks are not layered or deformed and garnet and clinopyroxene are fresh. Diamonds are 0.5–2 mm colorless and transparent octahedra, twinned-octahedra and irregularly shaped aggregates that occur at the grain boundaries of garnet and clinopyroxene, where commonly the morphology of diamond is controlled by the morphology of these minerals. The diamonds are variably surrounded by a fine-grained black material, consisting of fine phlogopite, apatite, carbonate and a Mg- and Al-rich silicate phase. This assemblage also occurs as thin vein networks throughout the eclogites, locally transecting both garnet and clinopyroxene crystals. Diamonds in the Jericho eclogites are also commonly mantled by phlogopite and these diamonds invariably have resorbed grain boundaries (Fig. 1b). However, a small population of diamond is in direct contact with neighboring garnet and clinopyroxene and a few sharp-edged, <0.5 mm diamonds occur as inclusions in garnet (Fig. 1c). Inter-connected networks of Ni-rich sulfide globules rimmed by phlogopite and carbonate are also present in the JDE (Fig. 1d). An additional discovery of this study is the occurrence of a tiny (~20 μm) garnet inclusion in diamond in eclogite JDE 03 (Fig. 1b), which is compositionally different from garnet in the host eclogite.

2. Analytical methods

We report the results on thirteen previously unstudied JDE from the Jericho kimberlite, and present new data on a suite of Group B and C eclogites, of which six (of fifteen total) were studied by Kopylova et al. (1999a). All JDE reported here are between 2–4 cm in diameter and were recovered during ore processing at the Jericho mine. Eclogite xenoliths were wrapped in multiple layers of plastic and coarsely crushed.

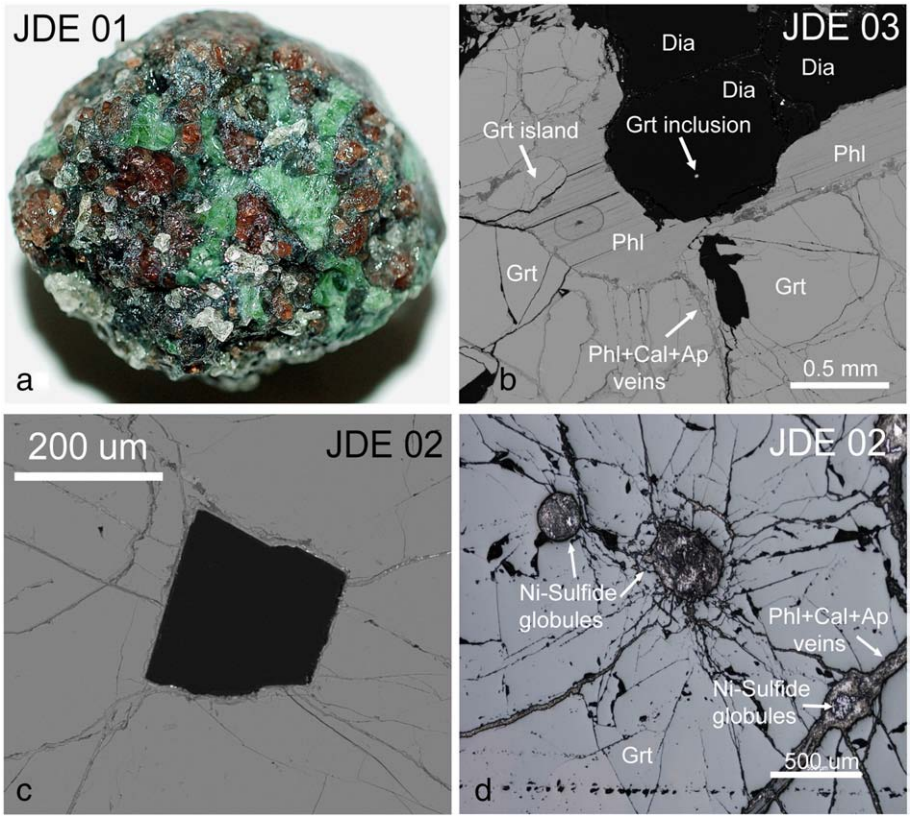

Fig. 1. (a) Photograph of Jericho diamond eclogite (JDE) 01. Xenolith is 4 cm wide. (b) Backscattered electron microprobe image of JDE 03 showing the textural relationship of diamond, pholgopite and garnet. The small light dot included in the central diamond is actually a garnet inclusion that was exposed during polishing of these sections, and is approximately 20 μm across. (c) Backscattered electron microprobe image of a diamond inclusion in garnet in JDE 02. (d) Reflected light photomicrograph showing pholgopite + apatite + calcite veins and associated Ni-sulfides. Grt = garnet, Phl = phlogopite, Cal = calcite, Ap = apatite, Di = diamond.

Inclusion-free garnet and clinopyroxene grains were handpicked in ethanol under a binocular microscope, mounted in epoxy, and analyzed for major elements using a JEOL 8900 electron microprobe at the University of Alberta. Analyses were performed using a 20 nA beam current and 20 kV accelerating voltage. Ten spots per mineral grain were analyzed in tracks across grains from rim to rim and a minimum of five garnet and five clinopyroxene were analyzed per xenolith. Major-element compositional data were also obtained for garnet, clinopyroxene and phlogopite in polished "thick" sections of the same xenoliths using the electron microprobe.

Trace-element compositions were obtained in both grain mounts (garnet and clinopyroxene) and thick sections (phlogopite) by laser ablation Quadrupole ICP-MS, using a New Wave Research Nd:YAG UP213 laser system coupled to a Perkin Elmer Elan 6000 Quadrupole ICP-MS. Laser spot size for all minerals was 160 μm and each ablation was 50 s in duration after 20 s of background counting times with a fluence of ~15 J/cm^2. Because of the small grain size, only one spot per mineral grain was analyzed, with a minimum of five grains of each mineral analyzed per xenolith. The NIST 612 standard was analyzed at the start and finish of each ablation session, and the ^{44}Ca content of each mineral, as determined by electron microprobe analysis, was used as an internal standard for calibration. Data were reduced using the GLITTER® software (van Achterbergh et al., 2001). The analytical precision for most elements at the 2σ level is between 7 and 40%, and is generally better than 10% with the higher uncertainties typical for elements present in low abundances (e.g. U, Th in garnet and HREEs in clinopyroxene). Further details on the techniques employed here can be found in Schmidberger et al. (2007).

Sr and Pb isotope compositions of clinopyroxene were obtained in-situ using the same laser system noted above coupled to a NuPlasma multicollector-ICP-MS. For clinopyroxene Sr isotope analyses, 160 μm diameter spots were ablated in clinopyroxene and data were collected using five Faraday detectors, following the procedure described in Schmidberger et al. (2003). Repeated analyses of a modern coral standard (Bizzarro et al., 2003) for Sr isotope investigations were completed during each analytical session and the ^{87}Sr/^{86}Sr ratios determined in this study (0.709115 ± 0.000071 and 0.709011 ± 0.000074) and from previously determined thermal ionization mass spectrometry analyses

Table 1
Geochemical and isotopic composition of the Jericho eclogites.

	JDE		JDE 03	44-9	Group B	JDE		44-9	Group B	JDE		44-9	Group B
	Grt avg.	Grt range	Grt D.I.	Grt	Grt avg.	Cpx avg.	Cpx range	Cpx	Cpx avg.	WR. avg.	WR. range	WR.	WR. avg
SiO_2	42.14	41.4–42.6	38.99	41.46	39.87	54.76	54.3–55.4	54.54	55.36	48.45	47.9–49.0	48.74	47.44
TiO_2	0.16	0.1–0.2	0.55	0.49	0.07	0.12	0.1–0.14	0.23	0.12	0.14	0.12–0.17	0.14	0.10
Al_2O_3	23.54	23.0–23.8	21.45	22.63	23.09	2.45	2.12–2.90	1.92	9.21	12.99	12.7–13.4	12.73	16.31
Cr_2O_3	0.56	0.30–0.72	0.10	0.54	0.06	0.32	0.13–0.40	0.71	0.08	0.44	0.22–0.56	0.45	0.07
FeO	8.65	8.25–10.4	17.36	9.19	16.73	2.21	2.07–2.81	3.30	3.41	5.43	5.17–6.63	5.20	10.45
MnO	0.39	0.37–0.43	0.39	0.37	0.30	0.08	0.07–0.08	0.10	0.03	0.24	0.23–0.26	0.23	0.17
MgO	20.20	19.0–21.2	13.16	20.07	11.64	16.62	15.8–17.0	17.20	10.63	18.42	17.8–18.9	18.94	10.98
CaO	4.13	3.91–4.31	7.38	4.42	8.31	20.46	20.0–20.9	19.89	15.78	12.30	12.0–12.6	12.48	11.97
Na_2O	0.05	0.04–0.06	0.13	0.06	0.05	1.68	1.40–1.92	1.63	5.03	0.87	0.73–0.97	0.91	2.48
K_2O	0.01	0.01–0.01	b.d.	b.d.	b.d.	0.01	b.d.–0.02	0.04	0.01	0.01	0.01–0.01	–	–
Total	99.83	98.8–101.1	100.08	99.24	100.13	98.70	98.5–99.5	99.56	99.66	99.36	98.3–100.3	99.83	99.98
Mg #	0.81	0.76–0.82	0.57	0.80	0.43	0.93	0.93–0.93	0.90	0.82	0.87	0.85–0.88	0.88	0.52
n/mode	13 xenos.		1 grain	7 grains	9 xenos.	12 xenos.		7 grains	9 xenos.	Mode: 50/50		50/50	Variable
V	248	229–283		211	52.5	541	465–693	258	201	395	347–482	235	127
Ni	22.7	19.8–25.6		27.9	16.9	235	187–267	193	242	129	102–1.46	110	76.9
Sc	102	87.5–113		102	48.4	25.6	24.6–27.0	102	16.6	63.4	56.1–70.0	102	21.5
Rb	0.15	0.02–0.3		b.d.	0.13	0.20	0.1–0.3	0.12	0.08	0.15	0.01–0.3	0.06	0.01
Ba	0.09	0.04–0.2		b.d.	0.22	2.89	1.0–5.8	0.39	0.23	1.52	0.6–2.9	0.19	0.05
Th	0.02	0.01–0.02		b.d.	b.d.	0.31	0.2–0.5	0.0	0.01	0.16	0.1–0.3	0.02	0.01
Nb	0.49	0.2–0.8		0.17	0.06	1.24	0.8–1.6	0.22	0.07	0.86	0.5–1.1	0.20	0.02
La	0.06	0.03–0.08		0.04	0.05	20.1	14–24.7	3.04	1.23	10.1	7.4–12.4	1.54	0.14
Ce	0.43	0.2–0.8		0.12	0.16	58.4	43.5–79.9	9.39	4.70	29.4	22.0–40.3	4.75	0.69
Pr	0.14	0.1–0.2		0.05	0.08	8.16	6.9–9.2	1.58	1.00	4.15	3.5–4.7	0.82	0.22
Pb	0.06	b.d.–0.1		b.d.	0.12	1.29	0.8–1.9	0.27	0.57	0.66	0.4–1.0	0.14	0.17
Sr	0.56	0.3–1.7		0.17	0.52	470	409–499	131	331	235	205–250	65.6	100
Nd	1.44	1.3–1.6		0.57	1.15	35.0	31.0–38.6	7.93	6.08	18.2	16.2–20.0	4.25	1.55
Sm	0.97	0.8–1.3		0.60	1.53	4.77	4.3–5.7	1.67	1.60	2.88	2.5–3.4	1.13	0.85
Zr	32.5	29.6–35.0		34.4	6.44	21.3	17.8–25.7	8.35	9.14	26.9	23.7–29.8	21.4	4.98
Hf	0.66	0.6–0.8		1.17	0.15	1.23	1.0–1.6	0.77	0.61	0.94	0.8–1.2	0.97	0.19
Eu	0.40	0.3–0.5		0.28	1.08	0.97	0.9–1.1	0.48	0.60	0.69	0.6–0.8	0.38	0.48
Gd	1.44	0.9–1.8		1.56	3.54	2.17	1.5–2.8	1.41	1.08	1.82	1.2–2.3	1.49	1.39
Tb	0.32	0.2–0.4		0.40	0.69	0.20	0.2–0.3	0.15	0.10	0.26	0.2–0.3	0.28	0.21
Dy	3.11	2.0–3.9		3.48	5.1	1.01	0.8–1.2	0.68	0.39	2.06	1.4–2.5	2.08	1.44
Y	24.8	21.8–29.4		15.7	25.4	3.90	3.4–4.6	1.99	0.99	14.3	12.6–17.0	8.82	5.74
Ho	0.94	0.7–1.1		0.76	1.10	0.17	0.1–0.2	0.10	0.04	0.55	0.4–0.7	0.43	0.26
Er	3.69	2.7–4.6		2.11	3.09	0.39	0.3–0.5	0.20	0.10	2.03	1.5–2.5	1.15	0.60
Tm	0.68	0.5–0.8		0.30	0.47	0.04	0.03–0.05	0.02	0.01	0.36	0.3–0.4	0.16	0.07
Yb	5.36	3.8–6.8		1.81	3.21	0.24	0.2–0.4	0.10	0.05	2.78	2.0–3.5	0.96	0.44
Lu	0.94	0.7–1.2		0.26	0.51	0.03	0.02–0.05	0.02	0.02	0.49	0.4–0.6	0.14	0.13
U	0.03	0.02–0.04		b.d.	0.03	0.06	0.03–0.08	0.01	0.021	0.04	0.02–0.06	b.d.	0.01
Eu_N*	0.98	0.7–1.2		0.74	1.23	0.81	0.7–0.9	0.92	1.33	0.32	0.3–0.4	1.09	0.39
La/Sm_N						2.65	2.0–3.5	1.14	0.22				
Lu/Gd_N	5.43	4.0–6.6		1.35	1.15								
$^{87}Sr/^{86}Sr$						0.7056	0.7047–0.7061	0.7032	0.7042				
$^{206}Pb/^{204}Pb$						18.63	18.54–18.68	18.75 ± 0.13	14.67–18.33				
$^{207}Pb/^{204}Pb$						15.58	15.5–15.73	15.55 ± 0.10	15.08–15.55				
n	9 xenos			7 grains	9 xenos	8 xenos	8 xenos	7 grains	9 xenos	8 xenos	8 xenos		9 xenos

Major element data in wt.%; trace element data in ppm. Average Jericho Group B eclogite data and clinopyroxene isotopic ranges from Smart et al., unpublished data.
Mg# calculated using Mg/(Mg + Fe); Eu* calculated using 2*Eu/(Sm + Gd), where all values are chondrite-normalized (McDonough and Sun, 1995).
W.R.: whole-rock eclogite composition calculated with estimated mode of 50% garnet, 50% clinopyroxene, see text for explanation; D.I.: diamond inclusion.

(0.709098 ± 0.000019, Bizzarro et al., 2003) are indistinguishable. Thus, a normalization factor was not required for the Sr isotope analyses of clinopyroxene. For Pb isotope analyses, clinopyroxene was ablated using a 320 µm by 320 µm raster pattern and a 160 µm diameter spot size. The Pb data were collected using three ion counters plus two Faraday detectors for Tl collection. The NIST 614 standard glass was analyzed for its Pb isotope composition at each session where measured $^{206}Pb/^{204}Pb$ deviated from the accepted values by less than 0.7%. The procedure employed here for Pb isotope data collection is similar to that described in Simonetti et al. (2005).

3. Results

3.1. Mineral chemistry

Table 1 lists the average garnet and clinopyroxene major- and trace element compositions of the JDE, one diamond-absent Group A eclogite (44-9) and an average Jericho Group B eclogite for comparison. Individual xenolith mineral chemistry can be found in Supplementary Tables 1 and 2. All mineral grains analyzed have homogeneous major element compositions that lack chemical zonation. Compared to Group B and C Jericho eclogites, garnets from the JDE investigated in this study have higher MgO (20.3 vs. 11.6 wt.%), and Cr_2O_3 (0.57 vs. 0.06 wt.%) contents (Fig. 2). The JDE also have higher TiO_2 (0.16 vs. 0.07 wt.%), Sc (102 vs. 48 ppm) and Zr (32 vs. 6.4 ppm) contents, and lower FeO (8.62 vs. 16.7 wt.%) and CaO (4.14 vs. 8.31 wt.%) contents than Group B eclogites. Garnets from high-MgO, diamond-absent eclogite 44-9 have a similar major element composition to garnets from the JDE, but have slightly higher TiO_2 (0.50 wt.%). Interestingly, the composition of the garnet inclusion in diamond in JDE 03 is similar to the Jericho Group B eclogites with much lower MgO (13.2 wt.%) and higher FeO (17.4 wt.%) and CaO (7.4 wt.%) than the garnet of the host eclogite.

Compared to the average composition of Group B eclogites, clinopyroxene from the JDE and eclogite 44-9 have significantly lower Al_2O_3 (2.5 vs. 9.2 wt.%) and Na_2O (1.7 vs. 5.0 wt.%) contents and higher MgO (16.6 vs. 10.6 wt.%), CaO (20.4 vs. 15.8 wt.%), Zr (21.6 vs. 9.1 ppm), Nb (1.23 vs. 0.07 ppm), V (546 vs. 201 ppm) and Cr_2O_3 (0.32 vs. 0.08 wt.%). Clinopyroxene from eclogite 44-9 has a major-element composition that is similar to the JDE clinopyroxene, but Group B-like Zr (8.3 ppm), Nb (0.22 ppm) and V (258 ppm). The major element compositions obtained here for garnet and clinopyroxene are similar to those previously reported for JDE (Cookenboo et al., 1998; Heaman et al., 2006).

Whole-rock compositions of the JDE were calculated using a visually estimated mode of 50% clinopyroxene and 50% garnet. Due to the small xenolith size (<4 cm in diameter) and coarse grain size in some cases (mineral grains up to 5 mm), modes are very difficult to determine. Variation of the mode by ±10% (e.g. 60% garnet, 40% clinopyroxene) can markedly change calculated whole-rock compositions, especially in terms of Al_2O_3, CaO, Na_2O and SiO_2 contents. For example, the Al_2O_3 content of eclogite JDE 01 increases from 12.7 to 14.8 wt.% when the garnet:clinopyroxene ratio is increased from 50:50 to 60:40. However, calculated whole-rock MgO and FeO contents are relatively independent of the mode estimate and distinctly different from Group B or C eclogites.

3.2. Rare earth elements

Chondrite-normalized REE plots for both garnet and clinopyroxene in the JDE are shown in Fig. 3 and are compared to Jericho Group B eclogites. Garnets in the JDE have enriched and fractionated chondrite-normalized HREE patterns (Lu_N ~30–54, $[Lu/Gd]_N$ ~5.8), where N indicates chondrite normalization using values from McDonough and Sun (1995), contrasting with the relatively flat HREE patterns of garnets from Group B and C eclogites ($[Lu/Gd]_N$ ~0.34—1.3) and 44-9 ($[Lu/Gd]_N$ = 1.4), a diamond-absent, Group A eclogite (Fig. 3a). Although less apparent, garnets from the JDE also have slight enrichments in Ce (Ce_N 0.38–1.23) and Pr (Pr_N 1.14–1.78) compared to garnets from the Group B eclogites (Ce_N 0.11–0.51, Pr_N 0.47–1.38). On a primitive mantle-normalized multi-element diagram (Fig. 4), the garnets from the JDE are distinguished from the Group B garnets by lack of a negative Zr-Hf anomaly and only a slight negative Ti anomaly.

Clinopyroxene from JDE (Fig. 3b) is markedly enriched in LREE (e.g. La_N = 78–103, La/Sm_N = 2.03–3.48) compared to Group B and C clinopyroxene (e.g. La_N = 0.2-17.6, La/Sm_N = 0.19–0.75). Calculated whole-rock chondrite-normalized REE plots, assuming a mode of 50% garnet and 50% clinopyroxene as described above, have sinusoidal shapes with enrichments in LREE and HREE, and relative depletions from Gd to Dy (Fig. 3c). Unlike the major elements, the REEs are not as sensitive to modes (Jerde et al., 1993; Aulbach et al., 2007) such that the overall sinusoidal-like pattern remains constant, but the degree of LREE or HREE enrichment varies with varying proportion of clinopyroxene or

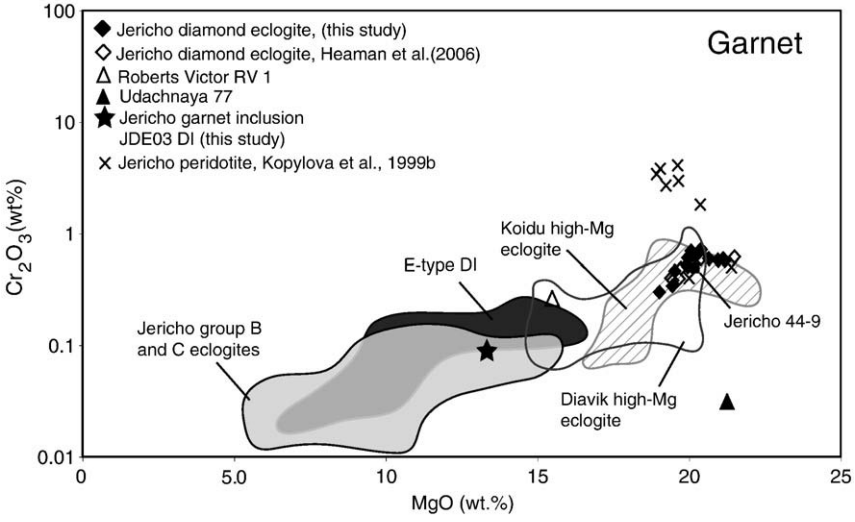

Fig. 2. MgO and Cr_2O_3 contents of garnets. The JDE garnets are compositionally similar in MgO to garnets from Jericho peridotite and pyroxenite (Kopylova et al., 1999b) and are clearly distinct from Jericho Group B and C garnets and also diamond inclusion garnets (Stachel et al., 2004). JDE garnets also compositionally overlap with high-MgO garnets from Koidu (Hills and Haggerty, 1989) and Diavik (Aulbach et al., 2007; Schmidberger et al., 2007). Garnets from two other high-MgO diamond eclogites from Udachnaya (77, Jacob and Foley, 1999) and Roberts Victor (RV 1 Jacob et al., 2005) are shown for comparison.

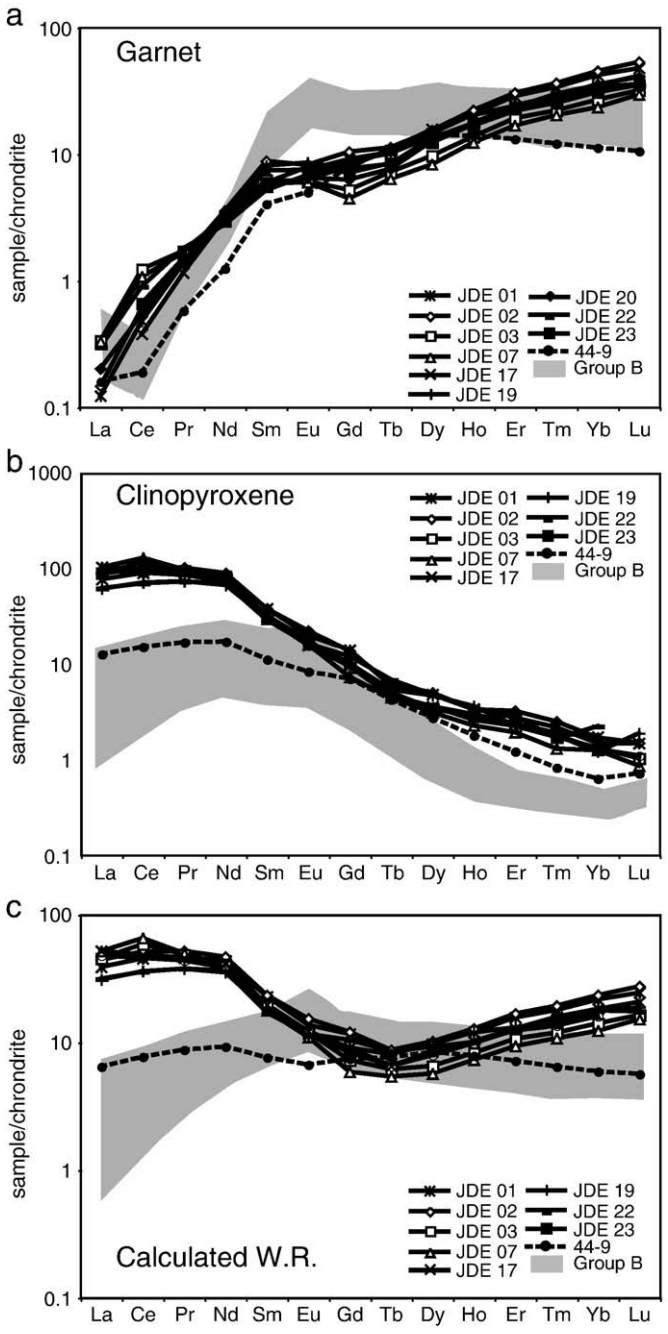

Fig. 3. Chondrite-normalized rare-earth element diagram for (a) Garnet, (b) clinopyroxene, and (c) calculated whole rock comparing all group A Jericho eclogites, including the JDE, to the Jericho Group B eclogites. Chondrite normalizing values are from McDonough and Sun (1995).

garnet, respectively. Although diamond makes up a significant portion of the mode, the primary versus secondary nature of the diamond is uncertain and was thus excluded from the whole-rock calculation.

3.3. Sr and Pb isotopes

The average Sr and Pb isotopic compositions of fresh clinopyroxene are listed in Table 1 and in Supplementary Table 2, and represent the average of four to nine grain analyses per xenolith. Clinopyroxene crystals from the JDE are compositionally homogeneous and have average Sr contents of 499 ppm. Excluding sample JDE 03, $^{87}Sr/^{86}Sr$ values (0.7057–0.7061) of JDE clinopyroxene are more radiogenic than the Jericho Group B and C eclogites (0.7032–0.7053). The JDE are also more radiogenic than the least radiogenic values reported for Jericho kimberlite whole-rock samples (present day ~0.7045; Kopylova et al., 2008) and an $^{87}Sr/^{86}Sr$ initial from a Jericho phlogopite megacryst Rb–Sr isochron (0.7053; Heaman et al., 2006). Of note, clinopyroxene grains from one diamond eclogite (JDE 03) record a range of $^{87}Sr/^{86}Sr$ values from 0.7039 to 0.7052; the variation in isotopic composition occurs both on an inter- and an intra-grain scale, and this range overlaps with the more radiogenic $^{87}Sr/^{86}Sr$ of the Group B and C clinopyroxene.

Clinopyroxenes contain on average 1.42 ppm Pb and have homogeneous Pb isotopic compositions ($^{206}Pb/^{204}Pb$ of 18.54–18.68 and $^{207}Pb/^{204}Pb$ of 15.46–15.73). Clinopyroxene from eclogite 44-9 has lower Sr (131 ppm) and Pb (0.27 ppm) contents and a range of less radiogenic $^{87}Sr/^{86}Sr$ (0.7028–0.7036) than the JDE, but identical $^{206}Pb/^{204}Pb$ and $^{207}Pb/^{204}Pb$. The generally uniform Pb isotopic composition of the JDE clinopyroxene contrasts with the variable isotopic composition of the Jericho group B and C eclogites ($^{206}Pb/^{204}Pb = 14.67–18.03$).

4. Discussion

Any model invoked to explain the formation of the Jericho high-MgO diamond eclogites must explain the following observations: 1) the high whole-rock MgO content in otherwise normal composition eclogites; 2) the sinusoidal whole-rock REE pattern, 3) the high Mg and Cr content and distinctive fractionated HREE pattern of eclogitic garnet; 4) the high LREE content and elevated $^{87}Sr/^{86}Sr$ of clinopyroxene; 5) the diamond-rich nature of the eclogite; and 6) the presence of a garnet inclusion in diamond that is markedly more Fe-rich than host garnet. However, before evaluating the origin of the high-MgO eclogites, it is important to assess the role of metasomatism in the formation of these eclogites.

4.1. Relative order of crystallization

The morphology of diamond appears in some cases to be controlled by the adjacent garnet or clinopyroxene grains, and thus likely formed after crystallization of the host eclogite. However, the presence of small diamond inclusions in garnet suggests that some diamond formation predated or was synchronous with the growth of garnet. Coarse-grained (up to 2 cm), low-Ba (0.42 wt.% BaO) phlogopite corrodes and fragments garnet and diamond (Fig. 1b) and therefore must have formed after diamond and garnet. Phlogopite formation in the JDE may also be related to the fine-grained veins that transect the host mineralogy of the xenoliths (Fig. 1b). Sulfide-bearing veins also formed late and may be linked to the phlogopite-carbonate-apatite veins suggested by similar vein assemblages.

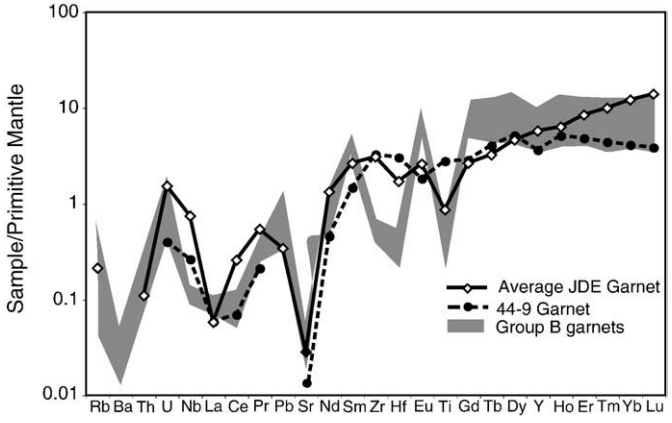

Fig. 4. Primitive-mantle normalized multi-element plot of garnet from the Jericho Groups A and B eclogites. Normalizing values are from McDonough and Sun (1995).

4.2. Evaluating the effects of metasomatism

4.2.1. Cryptic metasomatism

There are numerous studies of mantle xenoliths that have identified mineralogical, geochemical, and isotopic evidence of metasomatism (e.g. Erlank et al., 1987; Harte 1987). The JDE show evidence of at least two metasomatic events: a largely-cryptic event evidenced by the unique trace element and isotopic composition of clinopyroxene, and a later modal event, indicated by the growth of large phlogopite grains at the expense of other minerals.

Evidence for an early, cryptic metasomatic event includes the unique trace element and Sr isotope composition of clinopyroxene, the slight Ce and Pr enrichment in garnet, and the occurrence of diamond inclusions in garnet (Fig. 1c). JDE clinopyroxene is strongly LREE-enriched and interestingly has a trace-element pattern that is nearly identical to those reported for clinopyroxene from MARID and metasomatized garnet lherzolite xenoliths (Gregoire et al., 2002, 2003). These patterns are consistent with the interpretation that the clinopyroxene crystals either grew from or equilibrated with a LREE-enriched fluid or melt. In addition, the radiogenic $^{87}Sr/^{86}Sr$ of JDE clinopyroxene is similar to the high $^{87}Sr/^{86}Sr$ reported from metasomatized lherzolites and the MARID xenolith suite from South Africa (0.7039–0.7078, Kramers et al., 1983). The slightly higher Sr, Ba and Pb contents of the JDE clinopyroxene (Table 1) can also be explained by this metasomatic event. Well-formed diamond inclusions in garnet provide additional evidence of an early metasomatic event and also require that these eclogites experienced an early input of carbon, enabling diamond growth when conditions were favorable. It is plausible that this carbon addition to the eclogites occurred during the same metasomatic event recorded by clinopyroxene, but regardless of exact timing, the event must have occurred relatively early in eclogite formation. These geochemical and isotopic features of the JDE clinopyroxene are best explained by the involvement of a highly radiogenic $^{87}Sr/^{86}Sr$, LREE-enriched and carbon-bearing metasomatic agent. It is important to note that these features are absent in Jericho Group B and C eclogites and also in sample 44-9, the only Group A eclogite of this study that lacks diamond.

4.2.2. Modal metasomatism

Later episodes of modal metasomatism are indicated in the JDE xenoliths by the growth of large phlogopite crystals at the expense of garnet and diamond (Fig. 1b). In addition, all JDE contain veins with secondary growth of apatite, phlogopite, carbonate and Ni-sulfide (Fig. 1b and d), potentially linked to the infiltration of a carbonatite-like metasomatic agent. The timing of this metasomatism is currently poorly constrained but is considered to pre-date kimberlite magmatism and post-date eclogite formation, as the composition of the low-BaO (~0.42 wt.% BaO) phlogopite in the JDE is distinct from higher-BaO (up to 5.86 wt.% BaO) phlogopite in the Jericho kimberlite (Heaman et al., 2006). The fragmentation of eclogite and growth of large phlogopite crystals, corrosion of diamond at diamond–phlogopite contacts (Fig. 1b), and crystallization of fine grained phlogopite, apatite and carbonate along fractures all indicate a metasomatic overprint, subsequent to eclogite formation.

Unlike the carbonatite modal metasomatism discussed above, we consider the metasomatic overprint recorded by clinopyroxene to have occurred early in the history of these xenoliths, as clinopyroxene is also fragmented and locally transected by phlogopite–carbonate–apatite veins. As well, the lack of compositional zoning in both garnet and clinopyroxene argues against more recent (i.e. Jericho kimberlite related) metasomatic overprints. This early metasomatism was pervasive and produced Sr isotope compositions that are too radiogenic to permit direct derivation of these eclogites from pre-2.0 Ga oceanic crust or seawater-altered oceanic crust, which have $^{87}Sr/^{86}Sr$ of ~0.7013 and ~0.7040, respectively (Veizer and Compston, 1976; Workmann and Hart, 2005). It is noteworthy that the carbonatitic, high-density fluids (HDF) that occur as inclusions in fibrous diamonds from the Diavik (Klein-BenDavid et al., 2007, 2008) mine are also LREE-enriched and have radiogenic $^{87}Sr/^{86}Sr$ (up to 0.718). Therefore, similar fluids may have been widespread in the Slave lithospheric mantle and responsible for the observed cryptic metasomatism and growth of some diamond.

It should be noted that the radiogenic $^{87}Sr/^{86}Sr$ of the JDE is difficult to reconcile with carbonatite metasomatism as known 2.7 to 0.1 Ga North American carbonatites generally have lower initial $^{87}Sr/^{86}Sr$ (0.701–0.703; Bell and Blenkinsop, 1989) than the JDE. As well, JDE lack the Zr-Hf relative depletion commonly ascribed to carbonatite-like metasomatism (e.g. Yaxley et al., 1991) although such depletion may not be characteristic of primary mantle carbonatite melts (Foley et al., 2008).

The $^{206}Pb/^{204}Pb$ values of clinopyroxene in the JDE are very similar to the initial $^{206}Pb/^{204}Pb$ reported for Jericho eclogite rutile and garnet (Heaman et al., 2006) and within the range of values reported for South African Group I kimberlites (Smith, 1983). Thus, it is plausible that the agent responsible for cryptic metasomatism was a kimberlite-like fluid or magma. In summary, we propose that there are two metasomatic overprints that affected the JDE: an older, LREE-enriched metasomatic event and younger carbonatite-like modal metasomatic event. It is possible that both metasomatic events grew diamond, which may be the reason why these eclogites have such high modal diamond contents.

Although metasomatism has played a significant role in the history of the Jericho high-MgO diamond eclogites, the metasomatic agents discussed above cannot produce all the geochemical features of these xenoliths. Specifically, these agents alone cannot explain several of the compositional characteristics of garnet, including the fractionated HREE patterns, relatively high Cr_2O_3 and the absence of a Zr–Hf anomaly. For example, the effect of metasomatism on altered garnet from a Koidu high-MgO eclogite was investigated by Barth et al. (2002a) and although they report slight LREE-enrichment coupled with growth of ilmenite, phlogopite, amphibole, carbonate, sulfides and spinel in veins and along grain boundaries in these eclogites, they convincingly demonstrated that the HREE content of the metasomatized garnet was not perturbed. As discussed below, we propose that these features require a process not directly related to the metasomatism that profoundly changed the REE pattern and Sr isotope composition of clinopyroxene in these xenoliths.

4.3. Applicability of existing eclogite models to the JDE

Results from previous studies on Jericho eclogites (Schmidberger et al., 2005; Heaman et al., 2006) indicate that the basaltic composition, Group B and C eclogite xenoliths are most likely remnants of subducted oceanic crust — a finding that agrees with the widely invoked theory for mantle eclogite genesis (Jacob, 2004). However, it is difficult to reconcile the high Mg and Cr contents and other geochemical and isotopic characteristics of the JDE with an ocean-floor basalt protolith. Picritic or komatiitic protoliths can account for the high Mg contents but have much higher Fe and lower Al and Ca contents (e.g., Arndt, 1986; Barnes, 1985; Parman et al., 2004) than the JDE.

Another hypothesis proposed for the origin of mantle eclogites is that they represent cumulates of basaltic melts generated and crystallized at high pressure (e.g., O'Hara and Yoder, 1967; Smyth et al., 1989) and such an origin has been suggested for the JDE (Cookenboo et al., 1998). Although the uniform high-Mg and -Cr composition of most JDE garnets is broadly consistent with this hypothesis, there are several difficulties the model. Firstly, experiments (Herzberg and Zhang, 1997; Kawamoto and Holloway, 1997; Walter, 1998) indicate that high-pressure (>4 GPa) melts of peridotite are too low in Al and generally too high in Mg to match JDE compositions (Fig. 5). Secondly, the same experimental data indicate that olivine is an ubiquitous liquidus phase, yet all JDE and other high-Mg eclogites lack olivine

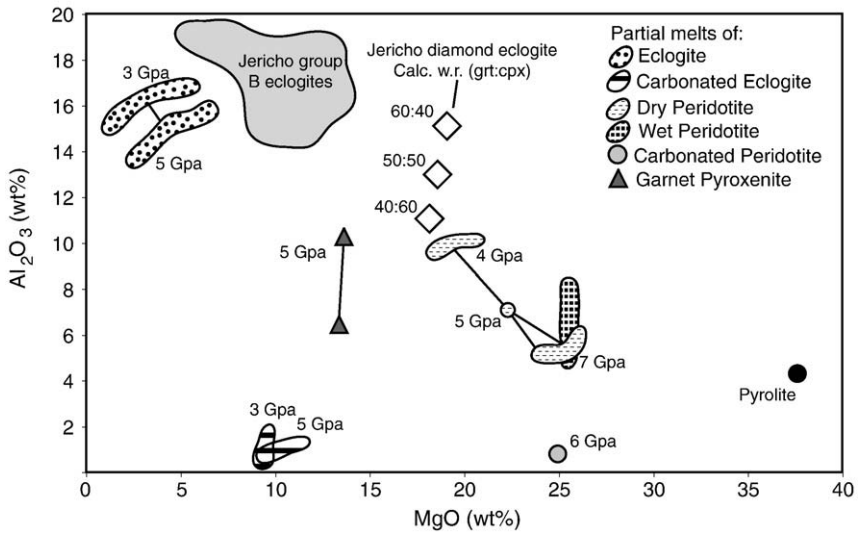

Fig. 5. Comparison of whole-rock calculated JDE and melts generated from various mantle lithologies. The variable whole-rock JDE composition is calculated by the mode percentage of garnet:clinopyroxene denoted beside each symbol. Melts generated from peridotite (Walter, 1998), wet peridotite (Kawamoto and Holloway, 1997) and carbonated peridotite (Brey et al., 2008) are too Al-poor and often Mg-rich to coincide with JDE compositions. The JDE are too Mg-rich to coincide with melts derived from garnet pyroxenites (Tuff and Gibson, 2007), eclogites (Spandler et al., 2008) or carbonated eclogites (Yaxley and Brey, 2004) and therefore did not crystalize from melts of common mantle lithologies. Pyrolite composition from McDonough and Sun (1995).

(Kopylova et al., 1999a; Barth et al., 2002a; Heaman et al., 2006). Partial melting of an olivine-free mantle lithology such as garnet pyroxenite can perhaps explain the absence of olivine in the JDE, but the JDE calculated whole-rock compositions (Table 1) also do not coincide with melt compositions of high-pressure partial melts of garnet pyroxenite (e.g. Tuff and Gibson, 2007) or those produced by mixing of partial melts of peridotite, pyroxenite and eclogite (Fig. 5). Thirdly, garnets formed in high-pressure peridotite or garnet pyroxenite melting experiments (Walter 1998; Kogiso et al., 2003; Tuff and Gibson, 2007) do not match JDE garnet compositions. Specifically, garnet produced from peridotite melting (e.g. Walter, 1998; Brey et al., 2008) has higher MgO (up to 27 wt.%) and Cr_2O_3 (0.9–2.3 wt.%) than JDE garnets. Garnets formed during partial melting of garnet pyroxenite have major-element compositions that are more akin to JDE garnets, but in general have lower MgO and Cr_2O_3 contents (Kogiso et al., 2003; Tuff and Gibson, 2007). Furthermore these garnets have flat to slightly fractionated $HREE_N$ ($[Lu/Gd]_N$~1.4; Tuff and Gibson, 2007) compared to the strongly fractionated HREE patterns ($[Lu/Gd]_N$~5.8) of the JDE garnets. We conclude therefore that a high-pressure cumulate origin is unlikely for this suite and an alternative model is required.

One possibility is that the high MgO content of the JDE was generated by infiltration of normal basaltic melt into peridotite and formation of a rock compositionally intermediate between basalt and peridotite. This type of basaltic metasomatism has been observed in peridotite xenoliths that have complexly zoned garnets (Burgess and Harte, 1999) and elevated garnet and clinopyroxene modes (Simon et al., 2003). However, such rocks contain significant olivine (e.g. Burgess and Harte, 1999) in contrast to the olivine-free nature of JDE. Moreover, chemical modeling of the basalt-peridotite mixtures indicates that these are too high in FeO (>8.5 wt.%) and too low in CaO (<10.5 wt.%) and Mg-number (~70) at the JDE whole-rock MgO content (19 wt.%) to be compatible with JDE whole-rock compositions (cf. Table 1).

5. Origin of Jericho high-MgO diamond eclogites

High-MgO diamond eclogites are rare worldwide but have been reported from South Africa, Russia and Finland (Jacob and Foley, 1999; Peltonen et al., 2002; Jacob et al., 2005). The JDE also share some compositional similarities with non-diamondiferous, high-MgO eclogites recovered at Koidu and Diavik eclogites (Fig. 2). We evaluate two possible explanations for the high-MgO content of the JDE: 1) metasomatic modification of Group B eclogites, and 2) derivation of Group A eclogites from a high MgO protolith, such as picrites or olivine gabbros (c.f. Barth et al., 2002a; De Stefano et al., 2009). Given the inability of these models to explain all the JDE features, we propose an alternative model that involves melt-facilitated equilibration of basaltic, Group B eclogite with surrounding peridotite.

5.1. Nature of the garnet diamond inclusion

The garnet diamond inclusion is important to the petrogenesis of the JDE as the inclusion is compositionally similar to the Jericho Group B garnets, albeit with slightly elevated Fe, Ti and Na. We interpret that the garnet inclusion represents the composition of the JDE *before* the process that created the high-Mg composition and attribute the higher Fe, Ti and Na to interaction with the diamond-forming agent during encapsulation. Although it is possible that the garnet diamond inclusion was formed by extensive metasomatism of a high MgO, Group A garnet by a HDF, modeling of known HDF compositions suggests that this type of interaction produces Ca-rich and Fe-poor compositions unlike the Fe-rich garnet diamond inclusion. Interaction of Group A eclogites with basaltic liquids can produce the appropriate Group B Fe-Mg composition, but this produces Al and Ca contents in the resulting modeled eclogite that are incompatible with Group B eclogite compositions. However, on the basis of the available data, we cannot discount the transformation of a JDE garnet to the Fe-rich garnet by complete equilibration with a Fe-rich melt/fluid, but it is important to note that there is no other record of such an interaction in the Jericho eclogites.

5.2. Metasomatic modification of basaltic eclogites

One explanation for the origin of the JDE could be that a high-Mg and trace-element enriched metasomatic agent modified Group B eclogites (compositionally similar to the garnet diamond inclusion described above) to the JDE composition. Two lines of evidence documented in other Jericho eclogites and diamond inclusions by De Stefano et al. (2009) support such model: 1) the range of compositions of diamond-inclusion garnets between Group A and B compositions; and 2) the recognition of secondary, high-Mg garnet and clinopyroxene in some Group B eclogites. There are, however, several difficulties with such a metasomatic conversion. The high MgO, secondary garnet in Group B eclogites form smaller polycrystalline aggregates around primary garnet cores (De

Stefano et al., 2009), which is in marked contrast to the relatively coarse and compositionally homogeneous mineral grains present in the JDE. Note that although the secondary garnet compositions reported by De Stefano et al. (in 2009) have higher MgO than the primary garnets, these secondary garnets are still not as magnesian as the JDE garnet compositions (Fig. 2).

Another difficulty with this metasomatic conversion is that it not only requires addition of Mg but also of relatively fluid immobile Ti, HREE and HFSE (e.g. Nb, Zr, Hf). As well, if an Mg-rich fluid is responsible for the Group B to A conversion then other elements concentrated in the agent would become enriched in the JDE. For example, the Mg-rich, high-density fluids involved in the growth of fibrous diamonds at Diavik (Klein-BenDavid et al., 2007, 2008) are variably enriched in K (15–20 wt.%), Na (2–20 wt.%) and Ba (7.7 wt.%) but none of these elements are enriched in the JDE (see Table 1). Therefore, Mg-rich HDF, like those documented at Diavik, were probably not responsible for the distinctive composition of the JDE. Interaction of Group B eclogites with a Mg-rich carbonatite magma could potentially explain some of the features of the JDE, including the phlogopite-apatite-carbonate vein assemblage and the LREE-enrichment of clinopyroxene. However, carbonatite metasomatism by itself cannot produce sufficient enrichment in Mg to account for the JDE compositions as most experimentally generated and mantle-derived primitive carbonatites (e.g. Wallace and Green, 1988; Tappe et al., 2006, respectively) have lower MgO contents than these eclogites. As well, carbonatite metasomatism cannot explain the HREE and HFSE enrichments present in the JDE.

Neither of the metasomatic agents discussed above can account for the REE patterns of the JDE. JDE garnets have fractionated, steeply sloping HREE (Fig. 3a) and to our knowledge, there is no mantle metasomatic process that can fractionate the HREE in garnet. Thus, it is difficult to envision how an Mg-rich metasomatic fluid/melt could have produced the fractionated HREE patterns of the JDE garnets. In this regard, garnet from Group A eclogite 44-9 has HREE patterns like those of Group B garnets rather than the fractionated HREE patterns of garnets in the JDE. If a single metasomatic process was responsible for modifying both the Mg contents and HREE patterns of the Group B garnets, then all Group A garnets, including 44-9, would be expected to display similar REE patterns.

5.3. Remnants of mafic lower oceanic crust

A second model for the origin of high MgO eclogites invokes an oceanic lower crustal protolith. Barth et al. (2002a) proposed this model for high-MgO Koidu eclogites, noting their normative compositions (40% plagioclase, 14% clinopyroxene, 12% orthopyroxene, and 29% olivine) are similar to some olivine gabbros and troctolites recovered from oceanic drill core (Aumento et al., 1977). They interpreted their eclogites as lower oceanic crust cumulates, which had originally crystallized at shallow levels, but had subsequently been subducted to great depth. The CIPW normative compositions of the Jericho Group A eclogites are very similar to the Koidu high-MgO eclogites, and Jericho eclogite 44-9 is almost identical to the Koidu high-Mg eclogites in terms of its REE composition (Fig. 6). As such, oceanic gabbro may be a viable protolith for the Jericho Group A eclogites.

There are, however, two problems with this hypothesis. Firstly, with the exception of two gabbro-norites (referred to as “eucrites” by Aumento et al., 1977), all other gabbros and troctolites reported from the DSDP and ODP studies (e.g. Hart et al., 1999; Bach et al., 2001) have Al_2O_3 contents that are too high (gabbros and olivine gabbros, 13.7–21.4 wt.%), MgO contents that are either too high (troctolites, >24 wt.%) or too low (gabbros and olivine gabbros, 7.1–13.1 wt.%), compared to the Jericho Group A eclogites. Secondly, due to their elevated plagioclase contents, almost all the aforementioned samples, including the two eucrites, have positive Eu anomalies on chondrite-normalized REE plots (Fig. 6). Thus, if the protoliths of the Jericho

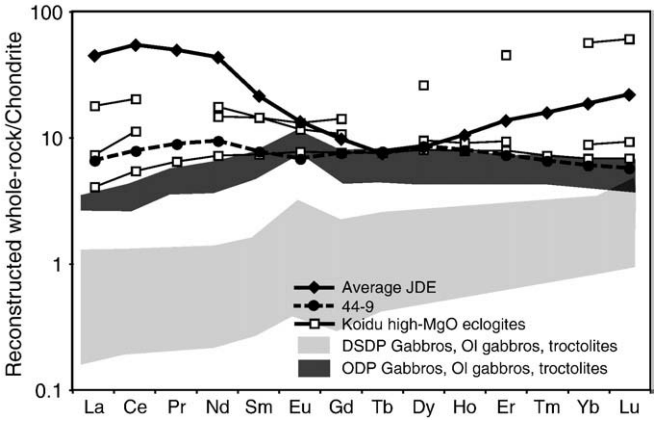

Fig. 6. Chondrite-normalized REE diagram of Jericho eclogite 44-9, average JDE, and three calculated whole rock Koidu high-Mg eclogites (Barth et al., 2002a). Also shown are fields for lower crust olivine gabbros and troctolites recovered from oceanic drilling expeditions. Ocean Drilling Program data from Hart et al. (1999) and Bach et al. (2001); Deep Sea Drilling Program data from Aumento et al. (1977).

Group A eclogites were in fact relatively plagioclase rich, as suggested by their normative compositions, their trace-element patterns should display clear positive Eu anomalies. However, Eu anomalies are conspicuously absent from all Jericho Group A eclogites (Fig. 3), conflicting with the low-pressure cumulate model.

5.4. Preferred model for the origin of high-MgO eclogites at Jericho

From the discussion of the two models above, it should be clear that finding a compositional match to the JDE has proven difficult. We therefore suggest a third model that focuses on the compositional similarity of garnet and clinopyroxene from JDE and those from Jericho mantle peridotites (e.g. Fig. 2), listed in Table 2. This new model proposes a melt-facilitated exchange of elements between neighboring eclogite bodies and mantle peridotite, envisioning a process similar to the mixed eclogite-peridotite melting experiments of Yaxley and Green (1998). In these experiments, equal amounts of peridotite and basaltic-composition eclogite were mixed and layered in the experimental charges and heated to temperatures of 1300–1500 °C at 3.5 GPa. Melts generated from the eclogite facilitated elemental exchange between eclogite and peridotite, producing a residual eclogite with Mg- and Cr-enriched garnet and clinopyroxene. The similarity between the major-element compositions of residual garnet produced in the Yaxley and Green (1998) experiments and JDE garnet is striking (Table 2).

5.4.1. Eclogite–peridotite elemental equilibration

It is possible that a similar hybridization process occurred in the Slave cratonic lithospheric mantle, whereby enclaves of basaltic, Group B-type eclogite (similar in composition to the garnet diamond inclusion), surrounded by peridotite underwent partial melting followed by equilibration with the surrounding mantle. Melt extraction alone from basaltic-composition eclogites cannot produce both the high MgO and low FeO observed in the JDE (e.g. Yaxley and Green, 1998; Yaxley and Sobolev, 2007) and therefore, the secondary, peridotite-equilibration step is required. Eclogite and pyroxenites have a lower solidus temperature than peridotite (Hirschmann and Stolper, 1996) and will therefore start to melt before surrounding peridotite during adiabatic ascent or thermal disturbance. During such an event, partial melting of carbon-bearing eclogite (carbon added during the precursor metasomatic event discussed above) generates a melt that facilitates relatively rapid diffusional Fe-Mg and Al-Cr exchange between restitic eclogite and surrounding peridotite. This exchange process may also be responsible for elevating the Sc, Zr and

Table 2
Geochemical comparison of JDE garnet and clinopyroxene to experimental and peridotitic minerals.

	Yaxley and Green, 1998 eclogite–peridotite experiments				Average Jericho coarse grt peridotite				Average Jericho diamond eclogite			
Run	9117 garnet	9117 cpx	520 garnet	520 cpx	Garnet		Cpx		Garnet		Cpx	
T (°C)	1300	1300	1500	1500								
Assemblage	Ga + cpx layer	Ga + cpx layer	Mixed	Mixed	$n=6$	2 s	$n=6$	2 s	$n=12$	2 s	$n=11$	2 s
SiO_2	42.3	53.4	42.7	54.3	41.33	0.5	54.47	0.6	42.15	0.7	54.74	0.8
TiO_2	0.7	0.4	0.5	0.2	0.16	0.2	0.15	0.1	0.16	0.0	0.12	0.0
Al_2O_3	23.2	5.7	23.0	6.2	21.59	1.2	2.19	0.5	23.50	0.5	2.51	0.5
Cr_2O_3	0.4	0.3	0.5	0.3	3.13	1.7	1.51	0.7	0.57	0.3	0.31	0.2
FeO	8.5	5.2	7.7	6.6	8.81	0.5	2.45	0.5	8.62	1.3	2.21	0.5
MnO	0.2	0.1	0.1	0.1	0.40	0.1	0.06	0.0	0.39	0.0	0.08	0.0
MgO	19.9	19.1	21.4	24.5	19.48	1.1	16.27	0.7	20.27	1.3	16.60	0.6
CaO	5.3	14.5	4.2	6.8	4.60	0.6	20.11	1.8	4.14	0.2	20.44	0.6
Na_2O	0.0	1.3	0.0	1.0	0.05	0.0	1.96	0.3	0.05	0.0	1.70	0.3
K_2O	0.0	0.0	0.1	0.0			0.06	0.0	0.00	0.0	0.01	0.0
Total	100.5	100.0	100.2	100.0	99.49	1.0	99.33	1.1	99.86	1.3	91.14	0.9

Data from Yaxley and Green (1998). All experiments at 3.5 Gpa. Data from Kopylova et al. (1999b).
Run 9117: equal amounts of basalt and pyrolite layered together.
Run 520: equal amounts of basalt and pyrolite homogeneously mixed.

Ni contents of garnets in the JDE relative to their Group B eclogite precursors.

If we consider eclogite 44-9 to be the most pristine Group A eclogite at Jericho, then the HREE patterns of garnet in the diamond eclogites require an additional process subsequent to emplacement at high pressure. One of the most enigmatic geochemical features of the JDE is the fractionated HREE in garnet. Previous element partitioning and experimental studies of peridotite and garnet pyroxenite compositions have yielded garnets with flat HREE patterns (e.g. Hauri et al., 1994; Harte and Kirkley, 1997; Johnson, 1998; Tuff and Gibson, 2007), similar to the patterns found in the garnets of 44-9, Group B eclogites and most other mantle eclogites worldwide. However, melting experiments of basaltic and gabbroic compositions at 3.0 to 4.5 GPa have residual garnets with variably fractionated HREE (e.g. Green et al., 2000; Pertermann et al., 2004; Yaxley and Sobolev, 2007), comparable to the HREE patterns of the JDE. Interestingly, a recent experimental study of high-pressure (ca. 6 GPa) partial melting of carbonated peridotite (Brey et al., 2008) also produced residual garnets with strongly fractionated HREE patterns ($[Lu/Gd]_N = 5.0\text{-}7.2$), nearly identical to those of the JDE garnets ($[Lu/Gd]_N = 4.0\text{-}6.6$).

Fig. 7 plots D_{Yb}/D_{Gd} in the experimental garnets versus the SiO_2 content of the coexisting melt. It appears that garnets coexisting with lower SiO_2, less-polymerized melts, such as carbonatitic melts, tend to have higher D_{Yb}/D_{Gd} than garnets coexisting with more silica-rich melts. This observation suggests that restitic garnets associated with carbonatitic or other low-silica melts are more likely to have strongly fractionated HREE patterns. Based on this experimental association, we speculate that the melts generated from the eclogite were silica-poor and responsible for the fractionated HREE patterns in the restitic garnets. These same melts may have facilitated elemental exchange between the eclogite enclaves and host peridotite.

5.5. Length-scale elemental equilibration in the mantle

The applicability of the eclogite–peridotite equilibration hypothesis to the formation of the JDE is critically dependent on the length-scales of elemental equilibration that might be expected in the mantle. Specifically, a small equilibration length-scale of only a few centimeters or decimeters would imply that this process, though possible, is volumetrically insignificant. Conversely, a larger equilibration length-scale would suggest a more extensive process that might well be reflected in the xenolith population. Length-scales can be estimated using bulk diffusion coefficients (D_{bulk} = weighted average of volume diffusion through mineral lattices and grain boundary diffusion) for relevant elements and an approximate time frame for mantle melting events (Brady, 1983; Joesten, 1983). In our calculations, we have used the experimentally measured diffusion rate of Mg in haplobasaltic melt (LaTourrette et al., 1996) to approximate the diffusion rate of Mg and Fe along melt-filled grain boundaries and the diffusion rate of Fe and Mg in garnet (Carlson, 2006) to approximate volume diffusion rates in eclogite minerals. The calculations indicate that, even at low melt fractions (1% melt), Mg–Fe equilibration length-scales (length $=\sqrt{D_{bulk}\,t}$) would be on the order of 0.7 to 5 m for melting events lasting 10^5 to 10^6 years at temperatures between 1200 and 1400 °C. Thus, provided that a grain boundary melt was present, minerals in Group B eclogite bodies located within a few meters of eclogite-peridotite interfaces would be expected to undergo significant amounts of Fe–Mg exchange with Mg-rich minerals in the adjacent peridotite. An appealing feature of this model is that it can account for the presence of the Fe-rich, Group B-like garnet inclusion in diamond in eclogite JDE03. The inclusion would reflect the primary garnet composition in the eclogite prior to the onset of partial melting and consequent Fe–Mg exchange with peridotite. Elements such as Al and Cr may also reflect exchange between eclogite and peridotite but the length-scale of this exchange is likely smaller because of the slower diffusion rate of trivalent relative to divalent cations in melts (LaTourrette et al., 1996).

6. Conclusions

Existing models that invoke a high-pressure cumulate or subducted oceanic crust origin cannot easily explain the unusual high-MgO

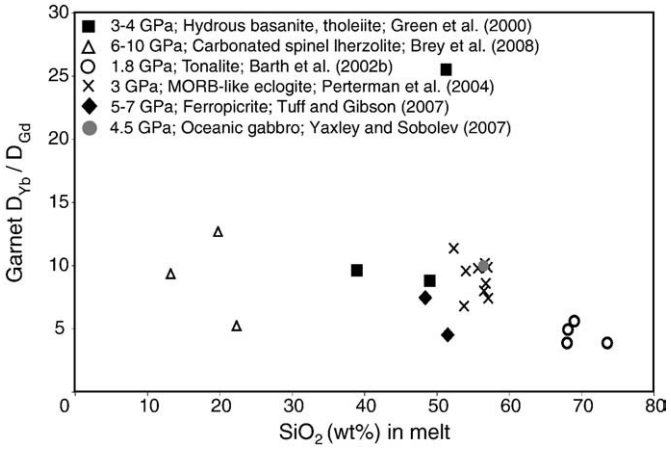

Fig. 7. The effect of melt polymerization on Gd/Yb partition coefficient ratios for garnets coexisting with partial melts produced from various lithologies. Garnets coexisting with silica-poor melts (i.e. Brey et al., 2008) have higher D_{Yb}/D_{Gd} and thus have more fractionated (steeply sloping) chondrite-normalized HREE than garnets in equilibrium with more silicic melts (i.e. Barth et al., 2002b). The experimental pressure and starting lithology are listed with the appropriate reference.

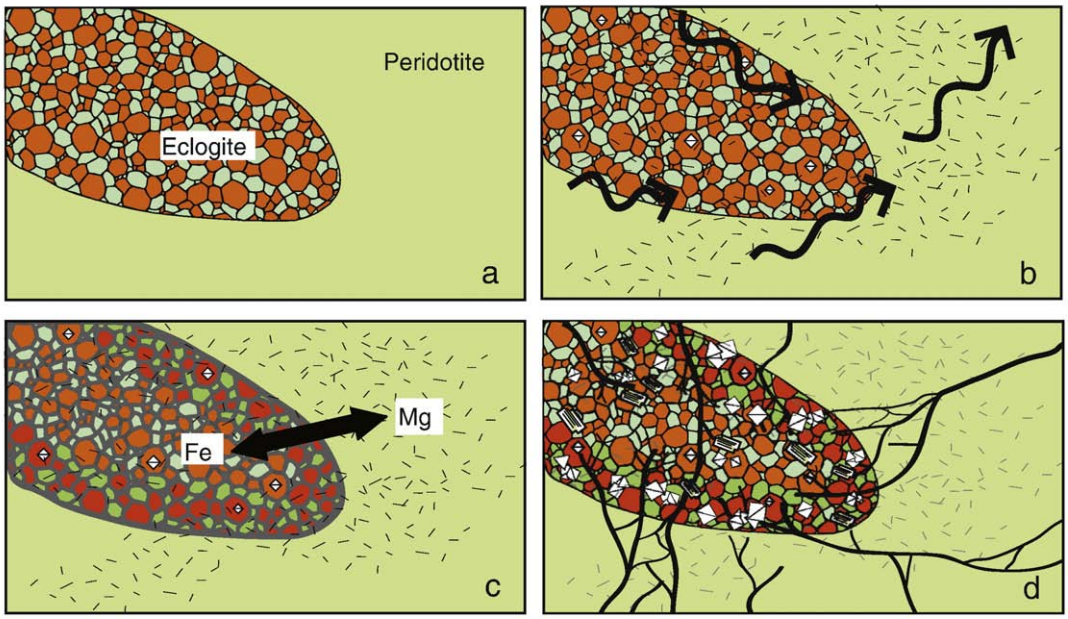

Fig. 8. Schematic diagram depicting the petrogenesis of the high-MgO Jericho diamond eclogites. (a) Emplacement of basaltic, Group B eclogites into peridotite (light green) in the northern Slave CLM. This event may be related to the Paleoproterozoic eclogite formation described by Heaman et al. (2006) and Schmidberger et al. (2005). (b) Metasomatism of Group B eclogites and peridotite (indicated by black arrows and dashes), which facilitated diamond growth, some of which occur as inclusions in garnets. Excluding diamond growth, this metasomatic event is largely cryptic, and is responsible for LREE-enrichment and the radiogenic Sr and Pb isotopic signatures observed in JDE clinopyroxene. The metasomatism must have occurred during garnet growth due to the diamond inclusions in garnet, and most likely occurred early in eclogite formation, perhaps during emplacement and eclogitization of a basaltic protolith. (c) Partial melting of Group B eclogites, represented by thick grey lines on eclogite mineral boundaries. A dacitic or carbonatitic melt, depending on the extent of eclogite metasomatism described in (b), is extracted from eclogite and facilitates Fe–Mg exchange between Group B eclogite and peridotite. The Fe–Mg elemental diffusion produces Mg-rich garnet and clinopyroxene (indicated by darker colors), where the degree of chemical exchange is more extensive closer to the peridotite–eclogite contact. The exact timing of partial melting and Fe–Mg exchange is uncertain, but encapsulation of a Group B garnet in diamond suggests this event may have been triggered by, or coeval with, diamond formation associated with the cryptic metasomatic event. (d) Modal metasomatism of the eclogite–peridotite assemblage by a potential carbonatitic–kimberlitic agent. This metasomatism produced coarse-grained phlogopite, potentially more diamond, and veins of fine-grained phlogopite, apatite, carbonate and sulfide in the JDE.

diamond eclogites at Jericho. Furthermore, we believe that previous models invoked to explain the generation of other high-MgO eclogites do not apply to the Jericho high-MgO suite. Rather, we propose a multi-stage, hybrid model to account for the mineralogical, geochemical, and isotopic features of these mantle eclogites, schematically represented in Fig. 8. The first stage involves emplacement of a Group B eclogite into the diamond stability field, producing a mixed low- to intermediate-MgO eclogite and peridotite mantle parcel. The second stage involves heterogeneous metasomatism of these mixed mantle lithologies by a carbon-bearing, LREE-enriched fluid. This metasomatic event was responsible for some diamond growth and the unusual geochemical (high LREE, Sr, Ba) and radiogenic strontium isotope composition recorded by clinopyroxene. After metasomatism, the basaltic composition eclogites experienced a partial melting event, which facilitated Fe–Mg exchange between the eclogite and the surrounding peridotite and produced the strongly fractionated HREE patterns in the restitic garnets. The final stage involved carbonatite-like metasomatism, and produced phlogopite, apatite, carbonate and facilitated more diamond growth.

Acknowledgements

This research was made possible by NSERC Discovery Grants to L.M. Heaman, T. Chacko and M. Kopylova. K.A. Smart acknowledges a NSERC post-graduate scholarship. We thank Tahera Diamond Corporation for access to the eclogite samples, S. Matveev for his assistance with the electron microprobe analyses, and D. Resultay for his innovative work in preparing thin sections of the diamond-bearing eclogites. We thank S. Aulbach, R. Luth, T. Stachel and S. Tappe for their comments and discussion that helped improve this manuscript. Thoughtful reviews by D. Jacob and one anonymous reviewer are greatly appreciated.

Appendix A. Supplementary data

Supplementary data associated with this article can be found, in the online version, at doi:10.1016/j.epsl.2009.05.020.

References

Arndt, N.T., 1986. Differentiation of komatiite flows. J. Pet. 27, 279–301.
Aulbach, S., Pearson, N.J., O'Reilly, S.Y., Doyle, B.J., 2007. Origins of xenolithic eclogites and pyroxenites from the central Slave Craton, Canada. J. Pet. 48, 1843–1873.
Aumento, F., Melson, W.G., Hall, J.M., 1977. Site 334. In: Aumento, F., Melson, W.G., Hall, J.M., et al. (Eds.), Initial reports of the deep sea drilling project, vol. 37. U.S. Government Printing Office, Washington, DC., pp. 239–287.
Bach, W., Alt, J.C., Niu, Y., Humphris, S.E., Erzinger, J., Dick, H.J.B., 2001. The geochemical consequences of late-stage low-grade alteration of lower ocean crust at the SW Indian Ridge: results form ODP Hole 735B (Leg 176). Geochim. Cosmochim. Acta 65, 3267–3287.
Barnes, S.J., 1985. The petrography and geochemistry of komatiite flows in the Abittibi Greenstone Belt and a model for their formation. Lithos 18, 241–270.
Barth, M.G., Rudnick, R.L., Horn, I., McDonough, W.F., Spicuzza, M.J., Valley, J.W., Haggerty, S.E., 2002a. Geochemistry of xenolithic eclogites from West Africa. Part 2: Origins of high MgO eclogites. Geochim. Cosmochim. Acta 66, 4325–4434.
Barth, M.G., Foley, S.F., Horn, I., 2002b. Partial melting in Archean subduction zones: constrains from experimentally determined trace element partition coefficients between eclogitic minerals and tonalitic melts under upper mantle conditions. Precambrian Res. 113, 323–340.
Bell, K., Blenkinsop, J., 1989. Archean depleted mantle: evidence from Nd and Sr initial isotopic ratios of carbonatite. Geochim. Cosmochim. Acta 51, 291–298.
Bizzarro, M., Simonetti, A., Stevenson, R.K., Kursziaukis, S., 2003. In situ $^{87}Sr/^{86}Sr$ investigation of igneous apatites and carbonates using laser ablation MC–ICP–MS. Geochim. Cosmochim. Acta 67, 289–302.
Brady, J.B., 1983. Intergranular diffusion in metamorphic rocks. Am. J. Sci. 283–A, 181–200.
Brey, G.P., Bulatov, V.K., Girnis, A.V., Lahaye, Y., 2008. Experimental melting of carbonated peridotite at 6–10 GPa. J. Pet. 49, 797–821.
Burgess, S.R., Harte, B., 1999. Tracing lithosphere evolution through the analysis of heterogeneous G9/G10 garnets in peridotite xenoliths I: major element chemistry. Proceeding of the 7th International Kimberlite Conference, Cape Town, vol. 1, pp. 66–80.
Carlson, W.D., 2006. Rates of Fe, Mg. Mn and Ca diffusion in garnet. Am. Mineral. 91, 1–11.
Coleman, R.G., Lee, E.D., Beatty, L.B., Brannock, W.W., 1965. Eclogites and eclogites: their differences and similarities. Geol. Soc. Amer. Bull. 76, 483–508.

Cookenboo, H.O., Kopylova, M.G., Daoud, D.K., 1998. A chemically and texturally distinct layer of diamondiferous eclogite beneath the Slave craton, Northern Canada. Extended Abstracts, 7th International Kimberlite Conference, Cape Town, pp. 164–166.
De Stefano, A., Kopylova, M.G., Cartigny, P., Afanasiev, V., 2009. Diamonds and eclogites of the Jericho kimberlite (Northern Canada). Contib. Min. Petrol. doi:10.1007/s00410-009-0384-7.
Ellis, D.J., Green, D.H., 1979. An experimental study of the effect of Ca upon garnet-clinopyroxene Fe–Mg exchange equilibria. Contrib. Mineral. Petrol. 71, 13–22.
Erlank, A.J., Waters, F.G., Hawkesworth, C.J., Haggerty, S.E., Allsopp, H.L., Rickard, R.S., Menzies, M.A., 1987. Evidence for mantle metasomatism in peridotite nodules from the Kimberley pipes, South Africa. In: Menzies, M.A., Hawkesworth, C.J. (Eds.), Mantle Metasomatism. InAcademic Press, London, pp. 221–311.
Foley, S.F., Yaxley, G.M., Rosenthal, A., Rapp, R.P., Jacob, D.E., 2008. Experimental melting of peridotite in the presence of CO_2 and H_2O at 40–60 kbar. 9th International Kimberlite Conference Extended Abstracts no. 156.
Green, T.H., Blundy, J.D., Adam, J., Yaxley, G.M., 2000. SIMS determination of trace element partitioning coefficients between garnet, clinopyroxene and hydrous basaltic liquids at 2–7.5 GPa and 1080–1200 °C. Lithos 53, 165–187.
Gregoire, M., Bell, D.R., Le Roex, A.P., 2002. Trace element geochemistry of phlogopite-rich mafic mantle xenoliths: their classification and their relationship to phlogopite-bearing peridotites and kimberlites revisited. Contrib. Mineral. Petrol. 142, 603–625.
Gregoire, M., Bell, D.R., Le Roex, A.P., 2003. Garnet lherzolites from the Kaapvaal Craton (South Africa): trace element evidence for a metasomatic history. J. Pet. 44, 629–657.
Hart, S.R., Blusztain, J., Dick, H.J.B., Meyer, P.S., Muehlenbachs, K., 1999. The fingerprint of seawater circulation in a 500-meter section of ocean crust gabbros. Geochim. Cosmochim. Acta 63, 4059–4080.
Harte, B., 1987. Metasomatic events recorded in mantle xenoliths: An overview. In: Nixon, P.H. (Ed.), Mantle Xenoliths. InJohn Wiley and Sons, United Kingdom, pp. 625–640.
Harte, B., Kirkley, M.B., 1997. Partitioning of trace elements between clinopyroxene and garnet: data from mantle eclogites. Chem. Geol. 136, 1–24.
Hauri, E.H., Wagner, T.P., Grove, T.L., 1994. Experimental and natural partitioning of Th, U, Pb and other trace elements between garnets, clinopyroxene and basaltic melts. Chem. Geol. 117, 149–166.
Heaman, L.M., Creaser, R.A., Cookenboo, H.O., 2002. Extreme enrichment of HFSE in Jericho eclogite xenoliths: A crypic record of Paleoproterozoic subduction, partial melting, and metasomatism beneath the Slave Craton, Canada. Geology 30, 507–510.
Heaman, L.M., Creaser, R.A., Cookenboo, H.O., Chacko, T., 2006. Multi-stage modification of the Northern slave mantle lithosphere: evidence from ziron-and diamond-bearing eclogite xenoliths entrained in Jericho kimberlite, Canada. J. Pet. 47, 821–858.
Helmstaedt, H., Doig, R., 1975. Eclogite nodules from kimberlite pipes in the Colorado Plateau-samples of subducted Franciscan type oceanic lithosphere. Phys. Chem. Earth 9, 95–111.
Herzberg, C., Zhang, J., 1997. Melting experiments on komatiite analog composition at 5 GPa. Am. Mineral. 82, 354–367.
Hills, D.V., Haggerty, S.E., 1989. Petrochemistry of eclogites from the Koidu Kimberlite Complex, Sierra Leone. Contrib. Mineral. Petrol. 103, 397–422.
Hirschmann, M.M., Stolper, E.M., 1996. A possible role for garnet pyroxenite in the origin of the "garnet signature" in MORB. Contrib. Mineral. Petrol. 124, 185–208.
Jacob, D.E., 2004. Nature and origin of eclogite xenoliths from kimberlites. Lithos 77, 295–316.
Jacob, D., Foley, S.F., 1999. Evidence for Archean ocean crust with low high field strength element signature from diamondiferous eclogite xenoliths. Lithos 48, 317–336.
Jacob, D.E., Jagoutz, E., Lowry, D., Mattey, D., Kudrjavtseva, 1994. Diamondiferous eclogites from Siberia: Remnants of Archean oceanic crust. Geochim. Cosmochim. Acta 58, 5191–5207.
Jacob, D.E., Bizimis, M., Salters, V.J.M., 2005. Lu–Hf and geochemical systematics of recycled ancient oceanic crust: evidence from Roberts Victor eclogites. Contrib. Mineral. Petrol. 148, 707–720.
Jagoutz, E., Dawson, J.B., Hoernes, S., Spettle, B., Wanke, H., 1984. Anorthositic oceanic crust in the Archean Earth. 15th Lunar Planet Sci. Conf. In, pp. 395–396. Abs.
Jerde, E.A., Taylor, L.A., Crozaz, G., Sobolev, N.V., Sobolev, V.N., 1993. Diamondiferous eclogites from Yakutia, Siberia: evidence for a diversity of protoliths. Contrib. Mineral. Petrol. 114, 189–202.
Joesten, R., 1983. Grain growth and grain-boundary diffusion in quartz from the Christmas Mountains (Texas) contact aureole. Am. J. Sci. 283–A, 233–254.
Johnson, K.T.M., 1998. Experimental determination of partition coefficients for rare earth and high-field-strength elements between clinopyroxene, garnet, and basaltic melt at high pressures. Contrib. Mineral. Petrol. 133, 60–68.
Kawamoto, T., Holloway, J.R., 1997. Melting temperature and partial melt chemistry of H_2O-saturated mantle peridotite to 11 GPa. Science 276, 240–243.
Klein-BenDavid, O., Izraeli, E.S., Hauri, E., Navon, O., 2007. Fluid inclusions in diamonds from the Diavik mine, Canada and the evolution of diamond-forming fluids. Geochim. Cosmochim. Acta 70, 723–744.
Klein-BenDavid, O., Pearson, D.G., Nowell, G.M., Cartigny, P., 2008. Origins of diamond forming fluids — constraints from a coupled Sr–Nd isotope and trace element approach. 9th International Kimberlite Conference Extended Abstracts no. 118.
Kopylova, M.G., Russell, J.K., Cookenboo, H., 1999a. Mapping the Lithosphere beneath the North Central Slave Craton. Proceeding of the 7th International Kimberlite Conference, Cape Town, vol. 1, pp. 468–479.
Kopylova, M.G., Russell, J.K., Cookenboo, H., 1999b. Petrology of peridotite and pyroxenite xenoliths from the Jericho kimberlite: implications for the thermal state of the mantle beneath the Slave craton, Northern Canada. J. Pet. 40, 79–104.
Kopylova, M., Nowell, G.M., Pearson, D.G., Markovic, G., 2008. Crystallization of megacrysts from kimberlites: Geochemical evidence from high-Cr megacrysts in the Jericho kimberlite. 9th International Kimberlite Conference Extended Abstracts no. 192.
Kogiso, T., Hirschmann, M.M., Frost, D.J., 2003. High-pressure partial melting of garnet pyroxenite: possible mafic lithologies in the source of ocean island basalts. Earth Planet. Sci. Lett. 216, 603–617.
Kramers, J.D., Roddick, J.C.M., Dawson, J.B., 1983. Trace element and isotope studies on veined, metasomatic and "MARID" xenoliths from Bultfontein, South Africa. Earth Planet. Sci. Lett. 65, 90–106.
Krogh Ravna, E., 2000. The garnet-clinopyroxene Fe^{2+}–Mg geothermometer: an updated calibration. J. Metamorph. Geol. 18, 211–219.
LaTourrette, T., Wasserburg, G.J., Fahey, A.J., 1996. Self diffusion of Mg, Ca, Ba, Nd, Yb, Ti, Zr, and U in haplobasaltic melt. Geochim. Cosmochim. Acta 60, 1329–1340.
McDonough, W.F., Sun, S.S., 1995. The composition of the Earth. Chem. Geol. 120, 223–253.
MacGregor, I.D., Manton, W.I., 1986. Roberts Victor eclogites: ancient oceanic crust. J. Geophys. Res. 91 (B14), 14063–14079.
O'Hara, M.J., Yoder, H.S., 1967. Formation and fractionation of basic magmas at high pressures, Scott. J. Geol. 3, 67–117.
Parman, S.W., Grove, T.L., Dann, J.C., De Wit, M.J., 2004. A subduction origin for komatiites and cratonic lithospheric mantle. S. Afr. J. Geol. 107, 107–118.
Peltonen, P., Kinnunen, K.A., Huhma, H., 2002. Petrology of two diamondiferous eclogite xenoliths from the Lahtojoki kimberlite pipe, eastern Finland. Lithos 63, 151–164.
Pertermann, M., Hirschmann, M.M., Hametner, K., Gunther, D., Schmidt, M.W., 2004. Experimental determination of trace element partitioning between garnet and silica-rich liquid during anhydrous partial melting of MORB-like eclogite. Geochem. Geophys. Geosyst. 5, 1–23.
Schmidberger, S.S., Simonetti, A., Francis, D., 2003. Small-scale Sr isotope investigation of clinopyroxenes from peridotite xenoliths by laser ablation MC–ICP–MS — implications for mantle metasomatism. Chem. Geol. 199, 317–329.
Schmidberger, S.S., Heaman, L.M., Simonetti, A., Creaser, R.A., Cookenboo, H.O., 2005. Formation of Paleoproterozoic eclogitic mantle, Slave Province (Canada): Insights from in-situ Hf and U–Pb isotopic analyses of mantle zircons. Earth Planet. Sci. Lett. 240, 621–633.
Schmidberger, S.S., Simonetti, A., Heaman, L.M., Creaser, R.A., Whiteford, S., 2007. Lu–Hf, in-situ Sr and Pb isotope and trace element systematics for mantle eclogites from the Diavik diamond mine: Evidence for Paleoproterozoic subduction beneath the Slave craton, Canada. Earth Planet. Sci. Lett. 254, 55–68.
Schulze, D.J., 1989. Constraints on the abundance of eclogite in the upper mantle. J. Geophys. Res. 94, 4205–4212.
Simon, N.S.C., Irvine, G.J., Davies, G.R., Pearson, D.G., Carlson, R.W., 2003. The origin of garnet and clinopyroxene in "depleted" Kaapvaal peridotites. Lithos 71, 289–322.
Simonetti, A., Heaman, L.M., Hartlaub, R.P., Creaser, R.A., MacHattie, T.G., Bohm, C., 2005. U–Pb zircon dating by laser ablation-MC–ICP–MS using a new multiple ion counting Faraday collector array. J. Anal. At. Spectrom. 20, 677–686.
Smith, C.B., 1983. Pb, Sr and Nd isotopic evidence for sources of southern Africa Cretaceous kimberlites. Nature 304, 51–54.
Smyth, J.R., Caporuscio, F.A., McCormick, T., 1989. Mantle eclogites: evidence of igneous fractionation in the mantle. Earth Planet. Sci. Lett. 93, 133–141.
Spandler, C., Yaxley, G., Green, D.H., Rosenthal, A., 2008. Phase relations and melting of anhydrous K-bearing eclogite from 1200–1600 °C and 3 to 5 GPa. J. Pet. 49, 771–795.
Stachel, T., Harris, J.W., 2008. The origin of cratonic diamonds — constraints from mineral inclusions. Ore Geol. Rev. 34, 5–32.
Stachel, T., Aulbach, S., Brey, G.P., Harris, J.W., Leost, I., Viljoen, K.S., 2004. The trace element composition of silicate inclusions in diamonds: a review. Lithos 77, 1–19.
Tappe, S., Foley, S.F., Jenner, G.A., Heaman, L.M., Kjarsgaard, B.A., Romer, R.L., Stracke, A., Joyce, N., Hoefs, J., 2006. Genesis of ultramafic lamprophyres and carbonatites at Aillik Bay, Labrador: a consequence of incipient lithospheric thinning beneath the North Atlantic Craton. J. Pet. 47, 1261–1315.
Tuff, J., Gibson, S.A., 2007. Trace-element partitioning between garnet, clinopyroxene and Fe-rich picritic melts at 3 to 7 GPa. Contrib. Mineral. Petrol. 153, 369–387.
van Achterbergh, E., Ryan, C., Jackson, S., Griffin, W.L., 2001. Laser-ablation-ICPMS in the earth sciences — Appendix 3 data reduction software for LA–ICP–MS. In: Sylvester, P. (Ed.), Mineralogical Association of Canada Short Course, vol. 29, pp. 239–243.
Veizer, J., Compston, W., 1976. $^{87}Sr/^{86}Sr$ in Precambrian carbonates as an index of crustal evolution. Geochim. Cosmochim. Acta 40, 905–914.
Wallace, M.E., Green, D.H., 1988. An experimental determination of primary carbonatite magma composition. Nature 335, 343–346.
Walter, M.J., 1998. Melting of garnet peridotite and the origin of komatiite and depleted lithosphere. J. Pet. 39, 29–60.
Workmann, R.K., Hart, S.R., 2005. Major and trace element composition of the depleted MORB mantle (DMM). Earth Planet. Sci. Lett. 231, 53–72.
Yaxley, G.M., Green, D.H., 1998. Reactions between eclogite and peridotite: mantle refertilization by subduction of oceanic crust. Schweiz. Mineral. Petrogr. Mitt. 78, 243–255.
Yaxley, G.M., Brey, G.P., 2004. Phase relations of carbonate-bearing eclogite assemblages from 2.5 to 5.5 GPa: implications for petrogenesis of carbonatites. Contrib. Mineral. Petrol. 146, 606–619.
Yaxley, G.M., Sobolev, A.V., 2007. High-pressure partial melting of gabbro and its role in the Hawaiian magma source. Contrib. Mineral. Petrol. 154, 371–383.
Yaxley, G.M., Crawford, A.J., Green, D.H., 1991. Evidence for carbonatite metasomatism in spinel peridotite xenoliths from western Victoria, Australia. Earth Planet. Sci. Lett. 107, 305–317.